Corrosion of S-Implanted Alloy 22 in 1 M NaCl Solutions

C. F. Windisch Jr.,[a,a] D. R. Baer,[a] R. H. Jones,[a] and M. H. Engelhard[a]

[a]*Pacific Northwest National Laboratory, Box 999, Richland, WA 99352, USA*

Abstract

Electrochemical and surface analysis studies on the passivation of Alloy 22, implanted with S at concentrations up to 2 at.%, in deaerated 1 M NaCl solutions indicated that, although there was very little reproducible influence from the S in the near-surface region on the corrosion current in the short term, the presence of S caused reproducible effect on the corrosion potential that was related to the amount of S present. In addition, there was strong evidence that S enriched on the surface of Alloy 22 during corrosion under normally passive conditions in deaerated NaCl solutions.

Keywords: alloy, XPS, ion implantation, polarization, passivity

1. Introduction

The barrier protecting the nuclear waste from the environment in the Yucca Mountain repository will be highly dependent on the nanometer thick passive film that forms on the metal waste packages. Even though the waste will be contained in a 25-mm thick vessel made from a very corrosion resistant Ni-Cr-Mo alloy, this corrosion resistance is the result of a nanometer thick oxide film that forms in aqueous solutions. There are several corrosion mechanisms, such as crevice, pitting and stress corrosion, that might potentially cause rapid failure of the waste package outer barrier but evidence suggests that the materials planned for the system can be designed to avoid these. The lifetime of the waste package will then be defined by the uniform corrosion rate and the long term stability of the nanometer thick passive film that readily forms on the proposed alloys. Therefore, mechanisms that could cause failure of the passive film during the long lifetime of the waste package outer barrier are very important.

Earlier work has shown that S has the propensity to enrich at metal surfaces and has been demonstrated to alter the stability of passive films on Ni and Ni-base alloys [1]. This enrichment could occur by thermal processing of the waste package outer barrier material, long-term aging at repository temperatures, diffusion from the grain boundary or inclusions intersecting the surface, adsorption from the environment and enrichment during corrosion. For a number of reasons,

adsorption from the environment and enrichment during corrosion are the two most likely mechanisms.

Several studies [2-9] have demonstrated that S, when present at the surface of metals, can assist the breakdown of passive films. Furthermore, in the case of S-enrichment due to passive corrosion, it was shown that enriched surface concentrations of S (compared to the impurity concentration in the bulk metal) were typically required to accelerate the corrosion process. It was also shown in these studies that the chemical state of S is critical to its effect on passive film stability. Reduced forms of S are more deleterious and oxidized forms less deleterious. An oxidation state of +4 was sufficient to eliminate the affect of S.

The accumulation of S over time has, in fact, been demonstrated for iron and nickel [10-12]. These concentrations could be achieved (for metals with typically low S-impurity levels) as a result of passive corrosion over long times under the assumption that the S accumulates at the surface and does not dissolve or oxidize. Based on several analyses, it is possible for a critical concentration of S (about 1 monolayer) to enrich on the surface of Alloy 22 (assuming a bulk S concentration of 100 ppm) in about 500 years at a corrosion rate of 0.01 μm/yr. Whether this enrichment will actually occur and whether it will cause a breakdown in the passive film, however, cannot be determined from the existing data base.

From the aspect of practicality, the mechanisms for this type of corrosion are not directly measurable by conventional immersion testing because the time-frame over which they are proposed to occur is too long. However, strategies are

available involving both sample preparation and testing that can accelerate measurements in a way that behavior over inaccessibly longer times can be reasonably approximated. One of these strategies, previously used in our laboratory to determine the effects of S on stress-corrosion cracking of Ni- and Fe-based alloys [10-12], used a combination of electrochemical and surface analysis measurement applied to metal samples that were ion-implanted with S to simulate the composition of S-impurity-enriched surfaces inside of a newly formed crack. The important characteristics of the S-implanted samples are discussed below.

The objective of this study was to examine the effects of high levels of S in the near-surface region on the passivity of Alloy 22 in deaerated 1 M NaCl solution. Near-surface concentrations of S up to 2 at.% were achieved in Alloy 22 test specimens by implanting them with S. The S-implanted samples were then evaluated in short-term electrochemical tests in the salt solution and subsequently analyzed with X-ray Photoelectron Spectroscopy (XPS) for film thickness and composition. Specimens tested included non-implanted and annealed Alloy 22 samples, samples implanted with S, and “blanks” implanted with Ar as an ion that would simulate the “damage” of S implantation without the chemical effect.

2. Experimental Procedure

Samples of Alloy 22, obtained from Haynes International (Kokomo, IN), had the following composition (in weight percent): 0.010 C, 0.29 Mn, 0.009 P, 0.001 S,

0.05 Si, 22.49 Cr, 12.58 Mo, 1.07 Co, 4.61 Fe, 0.19 V, 3.14 W, <0.01 Ti, Ni (remainder). These samples were cut into 1 cm^2 (0.4 cm thick) square samples and then ground and polished to a 1-μm diamond finish. Some of these were then sent to Core Systems/Implant Sciences, Inc (Sunnydale, CA) for implantation with S. Two implantation doses were chosen to achieve target peak compositions of 1 and 5 at.% S: (1) 50 keV and ion dose of $3.0x10^{15}$ ions/cm^2 to give expected S maximum of 1 at.% and (2) 50 keV and ion dose of $1.6x10^{16}$ ions/cm^2 to give an expected S maximum of 5 at.% based on calculated profiles. The peak maxima were expected at 20 – 25 nm under the sample surface. Ar ions were also implanted in other samples at a comparable dosage to a give similar concentration profile. The Ar-implanted samples were intended to serve as “control” samples that had no S, but a similar amount of implantation damage. Using the implanted materials along with specimens not implanted allows effects of damage and chemistry to be sorted out.

The profile of S concentration in the as-received samples that were implanted at the higher dosage is shown in Figs. 1a and 1b (different concentration scales). The S maximum is observed approximately 25 nm into the sample, as expected, but the peak S concentration was only 2 at.%, not the expected 5 at.%. Similarly, the lower dosage samples had relatively half of the expected value. Because the latter concentration was too low to be either representative or reliable, we elected to test only the high-dosage samples.

Consequently, all as-received S-implanted samples tested in this work had a S-concentration profile similar to that shown in Figs. 1a and 1b.

Since the effect of S concentration was important in this work, we also elected to “pre-sputter” some S-implanted samples using Ar ions in the XPS system prior to electrochemical testing. This caused the peak concentration of S to appear closer to the surface of the alloy sample so that there would be a greater likelihood of it having an effect. A S-concentration profile of one of these pre-sputtered samples is shown in Figs. 2a and 2b (different concentration and depth scales).

Electrochemical testing was performed using a PAR 273A potentiostat with PowerSuite software and a standard 3-electrode cell. The working electrode was the Alloy 22 specimen secured in a nylon sample holder that exposed 0.38 cm^2 surface area to solution. The counter electrode was a large-area Pt flag and the reference electrode was a saturated calomel electrode in a Luggin probe. Approximately 100 mL of solution was used for each test with the various compositions shown in Table 1, made up using reagent-grade chemicals and doubly-distilled water. All solutions were sparged with nitrogen and measurements were made under nitrogen in a glove box. For each electrochemical test, samples were equilibrated in solution for 1 h while obtaining potential-vs.-time data. After 1 h, the polarization curves were obtained. Potential was scanned from -250 mV cathodic to the original open-circuit (corrosion) potential to +300 mV-SCE. The scan rate was 1 mV/s.

The surface composition and oxidation state of the elements was measured using x-ray photoelectron spectroscopy (XPS) using a Physical Electronics Quantum 2000 Scanning ESCA Microprobe with a focused monochromatic Al Kα X-ray (1486.7 eV) source for excitation, a spherical section analyzer, and a 16-element multichannel detection system. The X-ray beam was 100 W with a 100 μm spot rastered over a 1.4 mm x 0.2 mm rectangle on the sample surface. The X-ray beam was incident normal to the sample and the X-ray photoelectron detector was at 45° off normal. Data were collected using a pass energy of 58.7 eV for S2p and 46.95 eV for all other elements. For the Ag 3d5/2 line, these conditions produced a full width at half maximum (FWHM) of 1.06 eV and 0.98 eV, respectively. The binding energy scale was calibrated using the Cu 2p3/2 feature at 932.62 ± 0.05 eV and Au 4f at 83.96 ± 0.05 eV for known standards. The relative amounts of the elements present on the surface were calculated using the Phi Multipak software program and standard surface sensitivity factors. As discussed in the results, the data can be further analyzed to extract useful information.

Argon ion sputtering was used to process the specimens in two different ways. Some ion-implanted specimens were pre-sputtered to expose the maximum amount of ion-implanted material. After the electrochemical tests, specimens were sputter profiled in order to determine composition and thickness of the surface layers and to monitor the presence and chemistry of any S present. Sputter depth profiling measurements were conducted in the XPS system using a

2 kV Ar ion beam rastered over areas as large as 3 mm by 3 mm for exposing implanted material. The sputter depths reported in this study are normalized to the sputter rate determined for identical conditions for a film of SiO_2 of known thickness. Although the sputter depths for the oxide layers on Alloy 22 may differ somewhat in sputter rate from SiO_2, this approach defines reproducible sputter conditions that allow accurate comparisons of relative thicknesses of the passive film layers.

3. Results and Discussion

The corrosion potential of each sample was monitored as a function of time and potentiodynamic polarization curves were obtained to determine the corrosion properties of Alloy 22 in deaerated 1 M NaCl solutions. For the reasons discussed above, the primary focus was the effect of S present in the surface region of the alloy as a result of ion implantation. However, a number of other parameters also had to be examined to separate their roles, if any, from that of S. First, since the pH of an unbuffered 1 M NaCl solution can change during corrosion, the effect of pH was determined by making measurements on solutions containing different pH buffers. Based on the results of these tests, two buffer solutions were selected for the majority of tests on the implanted samples. Second, the ion-implantation process creates atomic disorder in the implant region. Since this defect structure, in itself, may influence corrosion, we also tested Alloy 22 samples that were

implanted with the inert element Ar under conditions that were intended to give a similar implantation profile as the S-containing samples. By comparing the results of the S- and Ar-implanted samples, the effect of the implantation separate from that of S could be determined. Finally, since the S-implantation process results in a depth-dependent S concentration in the alloy, we chose to sputter most of the samples to achieve the maximum concentration of S at the sample surface. As shown in Figs. 1a and 1b, this amount corresponds to approximately 2 at.%. Since the sputtering process, separate from any S chemistry or other damage, may also induce corrosion effects, we studied Ar-implanted samples that had also been sputtered by similar amounts and specimens that had not been pretreated by sputtering. By comparing sputtered and not sputtered S- and Ar-implanted samples as well as non-implanted samples, we were able to distinguish the effects of S from those of the implantation or other processes.

3.1. Effect of pH

Corrosion potentials and potentiodynamic polarization curves were measured for non-implanted samples of Alloy 22 in 1 M NaCl solutions containing the different pH buffers listed in Table 1. These measurements were used to define test conditions for more detailed study. Corrosion potentials were measured in two ways: (1) as the open-circuit potential observed after 1-h immersion in the test solution and (2) from the potentiodynamic curves. The

corrosion potential values determined by these two ways differ for the reasons discussed below.

The corrosion potentials for the non-implanted samples measured after 1 hour equilibration in these tests are listed in Table 2 (along with results for the ion-implanted samples). The equilibration curves from which these values were obtained are given in Fig. 3. The polarization curves for the same samples, initiated after the 1-h equilibration, are given in Fig. 4 and the corrosion potentials determined from these curves are summarized in Table 3.

As shown in Tables 2 and 3, the corrosion potential was sensitive to the pH regardless of which approach was used. Values from the polarization curves are much more negative, however, and the trend is also different. For both approaches the values for the unbuffered and borate solutions are similar to each other. In both cases, the phosphate solutions gave the most negative values. The largest difference between the equilibration- and polarization-derived corrosion potentials was in the case of the KHP-buffered solutions, where the effect of polarization was to decrease the corrosion potential significantly relative to the other solutions.

The reason for the variation in the corrosion potentials from the two approaches can be understood as follows. As shown in Fig. 4, the polarization curves for the KHP and phosphate buffered solutions have a similar “peak” just anodic of the corrosion potential. This peak, which is larger for the more acidic buffer, is attributed to the reoxidation of products of the cathodic reaction that

occurred at potentials more negative than the corrosion potential. In acidic solutions, the cathodic reaction is $2H^+ + 2e \rightarrow H_2$. At 1 mV/s scan rate, apparently some of the reduced hydrogen (H_2 or adsorbed H_2 or H) is still resident near the working electrode and can be oxidized back to H^+ when the potential becomes anodic to the corrosion potential. This causes the "peak" that increases in current with decreasing pH. It also influences the potential of current reversal. Consequently, the corrosion potentials measured from the polarization curves are not strictly due to corrosion but result from a combination of corrosion and the products of the reduction reactions. The more negative values for the corrosion potentials extracted from the polarization curves are caused by the hydrogen reaction and, as expected, the influence of this reaction is greater at lower pH: i.e. KHP: -0.210 V (from equilibration) vs. -0.424 V (from polarization) compared to borate: -0.280 V (from equilibration) vs. -0.347 V (from polarization). The variation of the open-circuit potential with pH under acidic conditions is also consistent with the Nernst equation for the hydrogen reaction, yielding a slope of -0.0561 V pH^{-1}, compared to the expected -0.0591 value. This result means that our analysis of the corrosion potential in acidic solutions cannot use data from our polarization curves. Consequently, we elected to evaluate the behavior of the corrosion potential in this work (over all solution compositions) using the equilibration-derived values listed in Table 2.

At pH = 8.15, the cathode reaction is replaced by the reduction of dissolved O_2 or water, or, as is the case in these tests where the dissolved O_2 concentration

is very small, a mixture of the two. Since the potential for this reduction reaction does not follow the same pH dependence as H^+ reduction , the corrosion potential measured at pH = 8.15 does not follow the trend with pH for the more acidic solutions. As shown in Fig. 4, the polarization curve is different at pH = 8.15 and, as expected, is missing the anodic “peak” attributed to H re-oxidation.

The polarization curve for the unbuffered 1 M NaCl solution and the pH = 8.15 borate-buffered solution (Fig. 4) are very similar and their corrosion potentials are also essentially identical (as indicated in Table 2). This suggests that the unbuffered solution in the vicinity of the Alloy 22 electrode develops a pH near 8 at the corrosion potential during the polarization experiment. At potentials above approximately 0.0 V, the current for the borate-buffered solution is slightly higher, suggesting there is, once again, a gradual variation in local chemistry for the unbuffered solution, in this case when the potential is high enough.

The results of the pH-buffer studies suggest that there were at least two regions that should be considered for studying the effects of S: (1) at slightly higher pH (= 8.15) indicative of corrosion where local pH favors the neutral or high-pH cathodic reaction and (2) at slightly lower pH (= 3.67) where the corrosion process is accompanied by the hydrogen reduction reaction. It was anticipated that the two sets of experiments would also cover different regions of chemical activity for Alloy 22. In this way, its behavior in benign and slightly more aggressive environments, the latter presumably under the more acidic conditions, could be compared.

3.2. Comparison of Corrosion Potentials for Implanted and Non-Implanted Samples

As shown in Table 2, the corrosion potential (from equilibration measurements) was sensitive both to the type of implant and whether samples were pre-sputtered to the maximum-concentration depth of the implanted element or not. In general, the effect of both implantation and sputtering for a given solution pH appeared to be more pronounced at pH = 3.67 than at pH = 8.15. Much of our analysis, therefore, focused on the pH = 3.67 solutions. Implanting with either S or Ar shifted the equilibrium corrosion potential in the KHP-buffered solutions to more negative values relative to unimplanted samples. Furthermore, the effect of S was always greater (potentials were more negative) than the effect of Ar. Assuming that the role of implanting Ar is to induce damage only (no separate chemical effect from Ar), then this result suggests that (1) the implantation process itself activates the metal and (2) S has an additional activation effect due to its chemistry.

The sputtered samples for each implant also showed a greater negative shift than the unsputtered samples. This may mean that there is a relation between implant concentration at the surface and the size of the shift. For example, the unsputtered S-implanted samples have less than 1 at.% S at the surface (Figs. 2a and 2b), while the concentration is closer to 2 at.% for the

sputtered sample. More S at the surface gave a more negative corrosion potential. The same trend was observed for the samples implanted with Ar in the KHP solutions.

3.3. Comparison of Polarization Data for Implanted and Non-Implanted Samples

Comparisons of polarization data are limited in this paper to comparing the behavior of Ar-implanted and S-implanted samples that were sputtered to the implant-concentration maximum. Comparing these two sets of data shows the influence of S, distinct from any effects of both the implantation and sputtering processes. Data were also collected on implanted samples that were not sputtered to the maximum but these results were ambiguous because there may be an effect from the sputtering process, separate from any chemical effect from the implanted element. Arguably, samples that have been both implanted and similarly sputtered will have all conditions the same except for the identity of the implanted element.

As shown in the polarization curves in Figs. 5 and 6, the measured (passivation) currents for all conditions are generally very small, less than 1 microamp (with sample area about 0.38 cm^2). This means that there is no obvious enhancement of general corrosion (under passive conditions) from the S alone. XPS depth profile data is consistent with this as shown in Figs. 7 (a and b) and 8 (a and b). The extent of corrosion was very small leaving the S-implant layer

largely unaffected by the polarization experiments. The S concentration profile left after the sputtering step remained the same in the alloy after polarization. Careful scrutiny of the XPS depth profiles, however, reveals that the film thickness and its composition changed very slightly, however not in a way that could be correlated with the presence or concentration of S. Regardless of whether S was present or not, the films became slightly thinner due to polarization, by about half (Fig. 8a and 8b). Furthermore, the relative concentration of Cr-to-Ni in the thin oxide film increased. This latter effect is summarized in Fig. 9.

There are also some minor differences in the polarization curves as a function of the implanted element. As discussed previously, samples exhibited a more negative corrosion potential at pH = 3.67 than at higher pH. In the presence of S, the potential was even more negative. As shown in Fig. 5, this creates a region just positive of the corrosion potential that contains additional current from reversing the cathodic reaction, when it involves hydrogen. Between -0.4 V and -0.1 V, the currents are actually smaller when S is present compared to the Ar-implanted control, however it is unwise to scrutinize this region too closely because of the contribution of the re-oxidation reactions occurring beforehand at more negative potentials. There is also a slightly lower current for the S-implant at higher potentials, although the effect is small and may be within the uncertainties of the measurement.

As shown in Fig. 5, two runs were performed on the S-implanted sample at pH = 3.67. The first run showed a noisy current excursion between 0.05 and 0.1 V

that was not reproduced in the second experiment. Small negative excursions were also seen in the corrosion potential as a function of time for the second sample. The behavior is symptomatic of localized corrosion but, this could not be repeated or corroborated by surface analysis (or electron microscopy) results. According to the XPS data, the films were similar. The amount of charge passed during the largest current excursion for the first S-implanted sample in Fig. 5 is small, approximately 5×10^{-4} C or only 0.5% of the S inventory (left after sputtering) in the implanted layer. This suggests most of the S is still in the sample, despite the current excursion, consistent with the results of XPS analysis described above. If S has any impact on the corrosion behavior it appears to be irregular and transitory.

Polarization data on samples in the borate buffered (pH = 8.15) solution are shown in Fig. 6. These data also show the similarity between the Ar- and S-implanted (and sputtered samples), but this time with very little ambiguity. First, there was no anodic “peak” to confuse the data near the corrosion potential. The curves for the Ar- and S-implanted samples almost overlap near the corrosion potential and exhibit only a very slightly lower current (perhaps insignificant difference) for the S-implanted sample at higher potentials.

3.4. Sulfur Inventory and Chemistry

The electrochemical studies suggest only minor influences due to S on electrochemical measurements at the concentrations reported here (excluding the possibility of some local transient effects as noted earlier). However, the accumulation and/or oxidation of S near the surface of the alloys could impact the nature of the corrosion similar to other systems. In the case of Ni, long-term buildup of reduced S was shown to eventually alter the corrosion behavior [11]. In contrast, the oxidation of S minimized the impact on the corrosion of Fe [12].

The XPS measurements provide some information about both S buildup and oxidation. XPS data taken for S before and after exposure to solution or exposure to solution and polarization all show the S doublet to have a main photoelectron peak with a binding energy of 164.2 or slightly lower. Binding energies in this range are characteristic of elemental S and many metal sulfides. No peaks characteristic of oxidized S were observed for any sample or any of the experimental conditions examined in this study.

The lack of presence of oxidized S indicates either the non-oxidation of S in these studies or the removal of any oxidized S from the sample to the solution. The relative amplitude of the S photoelectron peak to those of the metal components provides an indication of S removal or buildup. Two different types of sample preparations were examined to test for S accumulation or removal. Corrosion tests were conducted on S-implanted samples with and without sputtering. In particular, for the samples with no sputtering, the S-to-metal ratio [at.%S/(at.%Ni+at.%Cr+at.%Mo)] before and after the electrochemical tests were

measured producing values of 0.019 and 0.032 respectively. If the possible impact of a carbon contamination layer is considered as described by Baker and Castle [13], the corrected values are 0.017 and 0.028. This measurement suggests that the relative concentration of S to metals in the film was increased by about 70% . Although the intensities of the S signals are small, they are very reproducible. A second test involves looking at the S-to-metal ratio for a sample sputtered to the maximum S in the sample relative to the sample after the electrochemical test. The last S signal collected during the sputter profile provided a S-to-metal atomic ratio with little or no influence of O (from oxides present) or C (contamination). The S-to-metal ratio taken after the exposure of the sample to solution had both O and C influencing the data. Nonetheless, we find that the initial S-to-metal ratio of the sputtered sample was 0.021 while the ratio after corrosion was 0.03 without the overlayer correction, and 0.0206 versus 0.0254 with a correction. This also suggests some increase in the near surface S (25-45%) after the corrosion process.

Although these increases are small, they were consistently measured and the differences are outside the scatter in the data. In considering differences between these two measurements it may be useful to remember that we are looking at the ratio of S to the sum Ni+Cr+Mo. For the as-received samples, the comparison involves S in the native oxide film that was involved in the implantation process and S in the oxide film after corrosion exposure. The relative amounts of Ni/Cr/Mo are 17/16/3 before electrochemical treatment and 14/19/3 after the

electrochemical treatments. There are changes in the Cr/Ni ratio as reported previously (Fig. 9) due to the electrochemical testing. However, the samples sputtered to the S max, with most oxygen removed, had significantly greater differences in the relative amounts of Ni/Cr/Mo, (55/29/14) in comparison to (13/19/6), after the electrochemical treatment. As expected the solution exposure produces a Cr-enriched oxide. The enrichment process may have some influence on the gain or loss of S over the short term.

It is useful to compare these results to what might be expected. What follows is a simple estimation of the magnitude of enhancement in S signal that might be expected based on the corrosion that has taken place. The total charge that has passed through the sample during electrical treatment is approximately 0.00075 C. This corresponds very roughly to consumption of 0.7 nm of material. If we assume that none of the sulfur in the 0.7 nm was removed and ask how much change in S signal would appear, we can use the exponential equation for XPS signals from Seah [14]. We first assume that no S is removed as 0.7 nm of material is dissolved. Assuming that the alloy contained S at a 2 at.% concentration initially and that the outer 0.7 nm becomes enriched to 4 at.% S during the electrochemical treatment (the S from the 0.7 nm of material dissolved remained in the outer 0.7 nm of material after electrochemical treatment) the ratio of corrosion enriched layer to the initial layer would be 1.25. Although there are many approximations in the calculation, the magnitude of the enrichment that would be expected is roughly the same as that observed. The XPS data suggest

much of the S that appears at the alloy surface remains near the surface during corrosion of the alloy in the conditions examined in this work.

The buildup of S near the surface of the implanted samples suggested by the above analysis seemed important, so we investigated it further by placing an as-received S-implanted specimen in 1 M NaCl, pH = 3.67, solution at open-circuit potential for twenty-nine days. Although the anodic current density at the open-circuit potential is not accurately known, it can be estimated to be approximately 1 to 2.5 x 10^{-7} A cm^{-2}. This current density for 29 days would expose between 7 and 17 x 10^{15} atoms cm^{-2} of S. Data collected during sputter profiles of a control sample and the sample exposed for twenty-nine days show that S does indeed accumulate in the surface region during solution exposure. Based on the differences in the S-to-metal ratios for the as-received sample and the sample exposed for 29 days (Fig. 10) during the sputter profile, and assuming that the sputter rate for the alloy/alloy-oxide layer is similar to that of SiO_2, the additional S accumulation near the surface was about 8 x 10^{15} atoms cm^{-2}.

The twenty-nine day open-circuit experiment confirms that S does accumulate on the surface and that it will build up with time. In spite of the many assumptions in the calculations of the amounts exposed and retained on the surface, they are similar enough to suggest that much of the exposed S is retained on the alloy surface when exposed to the solution conditions of this study. It should be noted that the implanted alloys have between 1 and 2 at.% S near the surface. Assuming that the base alloy contained about 10 ppm S, with the same

set of assumptions it would take 100 years to produce the surface enrichment we observed in about one month.

4. Conclusions

The objective of this study was to examine the effects of high levels of S in the near-surface region on the passivity of Alloy 22, a corrosion resistant Ni-Cr-Mo alloy, in deaerated 1 M NaCl solution. Near-surface concentrations of S up to 2 at.% were achieved in Alloy 22 test specimens by implanting them with S. The S-implanted samples were then evaluated in short-term electrochemical tests in the salt solution and subsequently analyzed with X-ray Photoelectron Spectroscopy (XPS) for film thickness and composition. Specimens tested included non-implanted and annealed Alloy 22 samples, samples implanted with S, and “blanks” implanted with Ar as an ion that would simulate the “damage” of S implantation without the chemical effect. A sample of S-implanted Alloy 22 was also exposed to solution for 29 days and analyzed for evidence of S accumulation at the surface over longer times.

Three primary findings resulted from this work: (1) There was very little, if any, reproducible influence from the S on the corrosion current in the short term when present in the surface layers of the alloy at concentrations up to 2 at.%. One experiment on a sample containing S exhibited a minor irregular current excursion in the polarization that suggested a localized corrosion process, but the event

could not be corroborated using other methods. (2) The presence of S caused a significant and reproducible negative potential offset to the alloy (separate from the effects of ion implantation) and the effect appears to be related to the amount of S present. (3) There is strong evidence that S can enrich on the surface of Alloy 22 during corrosion under normally passive conditions in deaerated solutions. The above results suggest that, although the short-term effects of S at 2 at.% or lower are minimal for Alloy 22 corrosion in deaerated 1 M NaCl, long-term exposure (100 years) of the alloy with bulk impurity concentrations as low as 10 ppm has the potential of raising surface-S concentrations higher than tested in this work and thereby influencing the corrosion process. This conclusion is based upon our observations that S appears to accumulate on the surface under all the conditions tested in this work and that there is a systematic shift in the open-circuit potential that depends on the amount of S. Studies on the impact of this buildup will require samples with even higher levels of surface-S than were tested in this work and should be the subject of additional study. It should also be noted that the role of dissolved oxygen on surface-S buildup needs to be studied in future work as well. In aerated environments, it is possible that the S may be significantly oxidized and removed (by dissolution) from the surface, thus ameliorating the long-term effects of the S-sulfur on corrosion.

Acknowledgment

The Pacific Northwest National Laboratory (PNNL) is operated by Battelle Memorial Institute for the U.S. Department of Energy under Contract DE-AC06-76RLO 1830. Funding for this work was provided by the Office of Civilian Radioactive Waste Management of the U.S. Department of Energy.

References

[1] R. H. Jones and C. F. Windisch Jr., *Surface Enrichment of Sulfur and Phosphorous on Alloy 22 and Implications for Long-Term Passivity,* Technical Report No. PNNL-15173, Pacific Northwest National Laboratory, Richland, WA 99352 (2005).

[2] T. W. Farrer and F. Wormwell, *Chem. Ind.*, 106 (1953).

[3] D.D. MacDonald, B. Roberts and J.B. Hyne, *Corrosion. Sci.*, 18, 411 (1978).

[4] H. Okada, Y. Hosoi and K. Yamamoto, *J. Electrochem. Soc.,* 12, 2036 (1971).

[5] P. Marcus, N. Barbouth and J. Oudar, *Comptes Rendus Hebdomadaiares Des Seances De L Academie Des Sciences Series*, C280, (19), 1183 (1975).

[6] J. Oudar and P. Marcus, *Appl. Surf. Sci*. 3, 48 (1979).

[7] P. Marcus and J. Oudar, *Fundamental Aspects of Corrosion Protection by Surface Modification*, E. McCafferty, C.R. Clayton and J. Oudar, Eds., The Electrochemical Soc., Pennington, NJ , 173 (1984).

[8] P. Marcus, A. Teissier and J. Oudar, *Corrosion. Sci.*, 24, 259 (1984).

[9] P. Marcus, “Sulfur-Assisted Corrosion Mechanisms and the Role of Alloyed Elements,” in *Corrosion Mechanisms in Theory and Practice*, P. Marcus, Ed., Marcel-Dekker, 287 (2000).

[10] Baer, D.R. and M.J. Danielson, *J. Vac. Sci. Technol. A*, 5 (4), 1147 (1987).

[11] Danielson, M.J. and D.R. Baer, *Corrosion Sci.*, 29, p. 1265 (1989).

[12] C.F. Windisch, Jr., D.R. Baer and M.H. Engelhard, *J. Electrochem. Soc.*, 141, 2343 (1994).

[13] J. E. Castle and M. A. Paker, *J. Elec Spec & Related Phenomena*, 105, 245 (1999).

[14] M. P. Seah in *Practical Surface Anaysis*, 2nd Ed., Edited by D. Briggs and M. P. Seah, Wiley Publishing, New York, 1992.

Figure Captions

Fig. 1. XPS depth profile for as-received S-implanted Alloy 22 sample. (a) and (b) are at different concentration scales.

Fig. 2. XPS depth profile for untested S-implanted Alloy 22 sample after sputtering with Ar ions to achieve approximately the S-concentration maximum at the surface. (a) and (b) are at different concentration and depth scales.

Fig. 3. Corrosion potential vs. time for non-implanted Alloy 22 samples in deaerated 1 M NaCl solutions with different pH buffers. Samples do not have S or Ar in them. The corrosion potential after 1 h immersion is noted.

Fig. 4. Potentiodynamic polarization curves for Alloy 22 containing non-implanted elements in deaerated 1 M NaCl solutions with different pH buffers. Samples do not have S or Ar in them. Scan rate was 1 mV/s.

Fig. 5. Potentiodynamic polarization curves for Alloy 22, implanted with Ar and S (duplicate runs for S) and subsequently sputtered to the implant-concentration maximum, in deaerated 1 M NaCl solutions buffered to pH = 3.67 with KHP.

Fig. 6. Potentiodynamic polarization curves for Alloy 22, implanted with Ar and S and subsequently sputtered to the implant-concentration maximum, in deaerated 1 M NaCl solutions buffered to pH = 8.15 with borate.

Fig. 7. XPS depth profile for S-implanted Alloy 22 samples (a) as-received and (b) after sputtering with Ar ions (to achieve approximately the S-concentration maximum at the surface), followed by equilibration at the corrosion potential for 1 h and electrochemical polarization. This scale shows the variation of Cr concentration near the surface.

Fig. 8. XPS depth profile for S-implanted Alloy 22 samples (a) as-received and (b) after sputtering with Ar ions (to achieve approximately the S-concentration maximum at the surface), followed by equilibration at the corrosion potential for 1 h and electrochemical polarization. This scale shows variations closer to the surface than Fig. 7.

Fig. 9. Variation of the Cr/Ni atom ratio near the surface for different Alloy 22 samples.

Fig. 10. Depth profile showing the ratio of S-to-metal concentrations as a function of depth for a control sample (S-implant) and S-implanted sample exposed to

solution for 29 days. An excess amount of S was accumulated in the surface region of the sample during the 29 days in solution.

Table 1

pH Buffered Solutions Used in This Work

pH Buffer	Measured pH	Composition
Unbuffered	6.5 (Initial)	1 M NaCl
KHP	3.67	1 M NaCl, 0.05 M Potassium Hydrogen Phthalate
Phosphate	6.36	1 M NaCl, 0.025 M KH_2PO_4, 0.025 M Na_2HPO_4
Borate	8.15	1 M NaCl, 0.0125 M Borax, 0.02 M HCl

Table 2

Corrosion Potentials Measured after 1 h Immersion in Solution

Solution	pH	Corrosion Potential after 1 h, V vs. SCE				
		No Implant or Sputtering	Implanted w/o Sputtering		Implanted and Sputtered	
			Ar	S	Ar	S
1 M NaCl (Unbuffered)		-0.260, -0.275*		-0.330		
1 M NaCl + KHP Buffer	3.67	-0.210	-0.235, -0.235*	-0.245	-0.254	-0.270
1 M NaCl + Phosphate Buffer	6.36	-0.350				
1 M NaCl + Borate Buffer	8.15	-0.270, -0.280*			-0.299	-0.312

*Duplicate run.

Table 3

Corrosion Potentials from Polarization Curves

Solution	pH	Corrosion Potential from Polarization, V vs. SCE				
		No Implant or Sputtering	Implanted w/o Sputtering		Implanted and Sputtered	
			Ar	S	Ar	S
1 M NaCl (Unbuffered)		-0.347		-0.403		
1 M NaCl + KHP Buffer	3.67	-0.424	-0.365, -0.367*	-0.451	-0.402	-0.466, -0.449*
1 M NaCl + Phosphate Buffer	6.36	-0.575				
1 M NaCl + Borate Buffer	8.15	-0.347			-0.349	-0.365

*Duplicate run.

Fig. 1

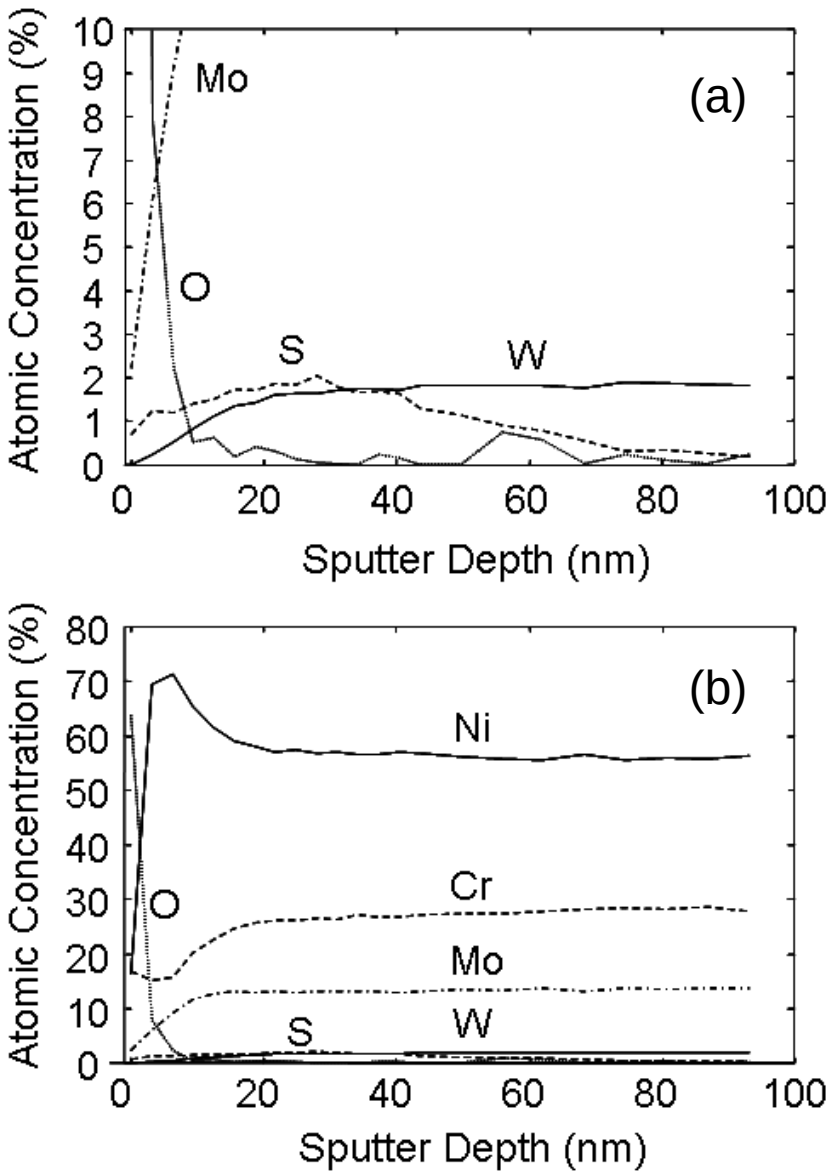

Fig. 1. XPS depth profile for as-received S-implanted Alloy 22 sample. (a) and (b) are at different concentration scales.

Fig. 2

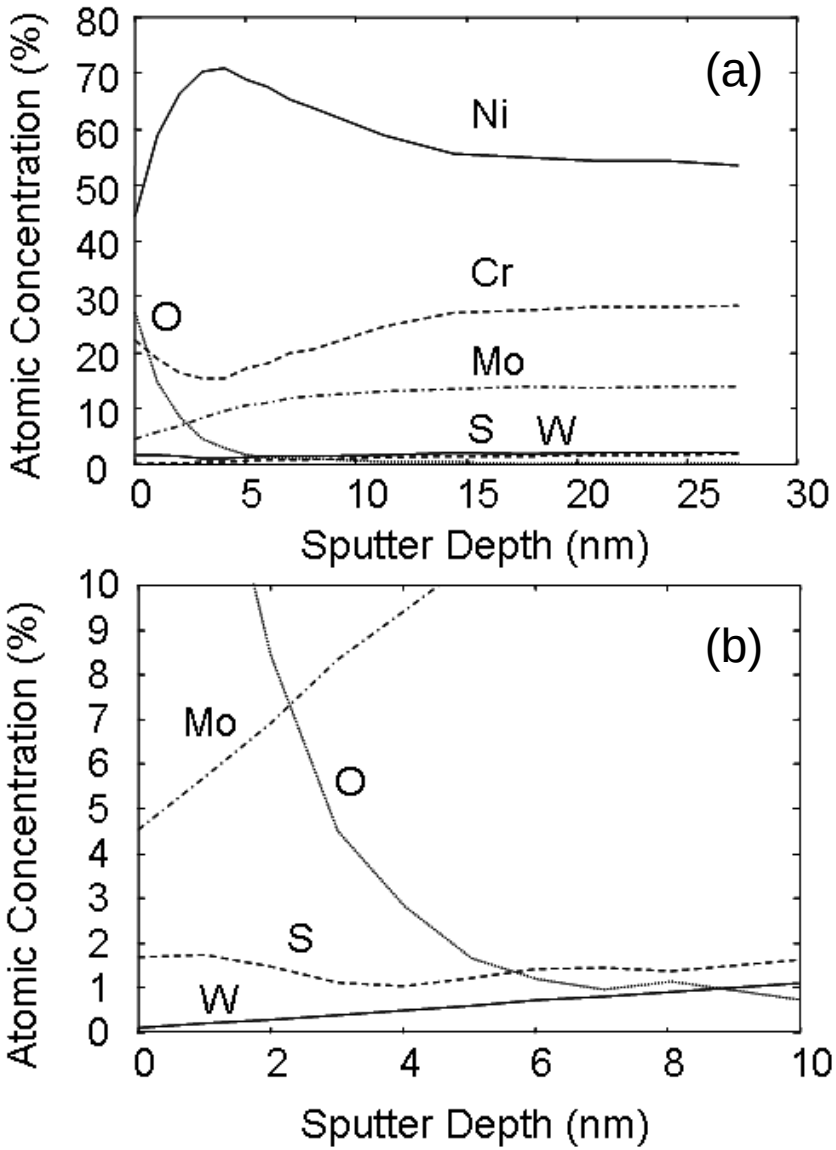

Fig. 2. XPS depth profile for untested S-implanted Alloy 22 sample after sputtering with Ar ions to achieve approximately the S-concentration maximum at the surface. (a) and (b) are at different concentration and depth scales.

Fig. 3

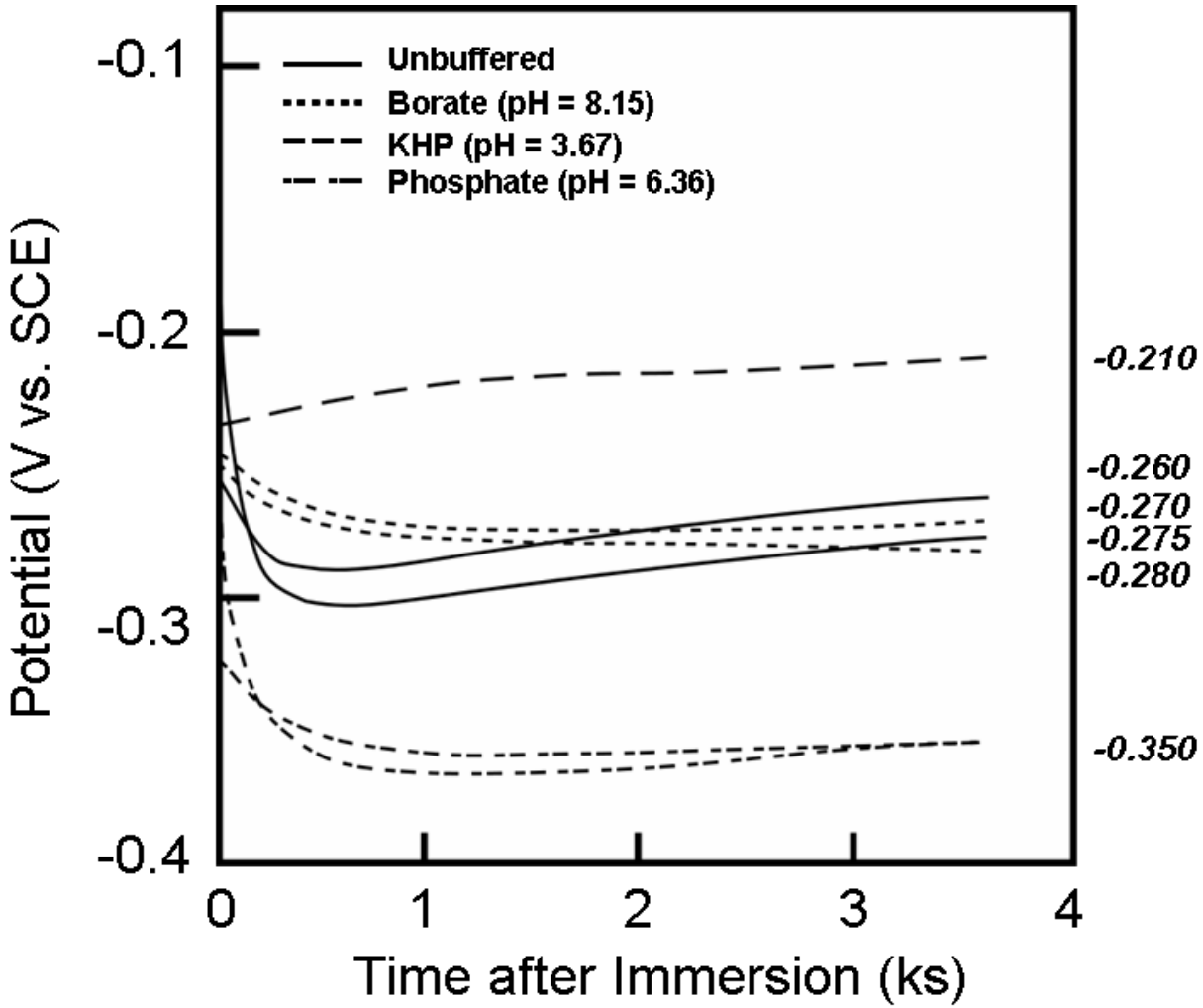

Fig. 3. Corrosion potential vs. time for non-implanted Alloy 22 samples in deaerated 1 M NaCl solutions with different pH buffers. Samples do not have S or Ar in them. The corrosion potential after 1 h immersion is noted.

Fig. 4

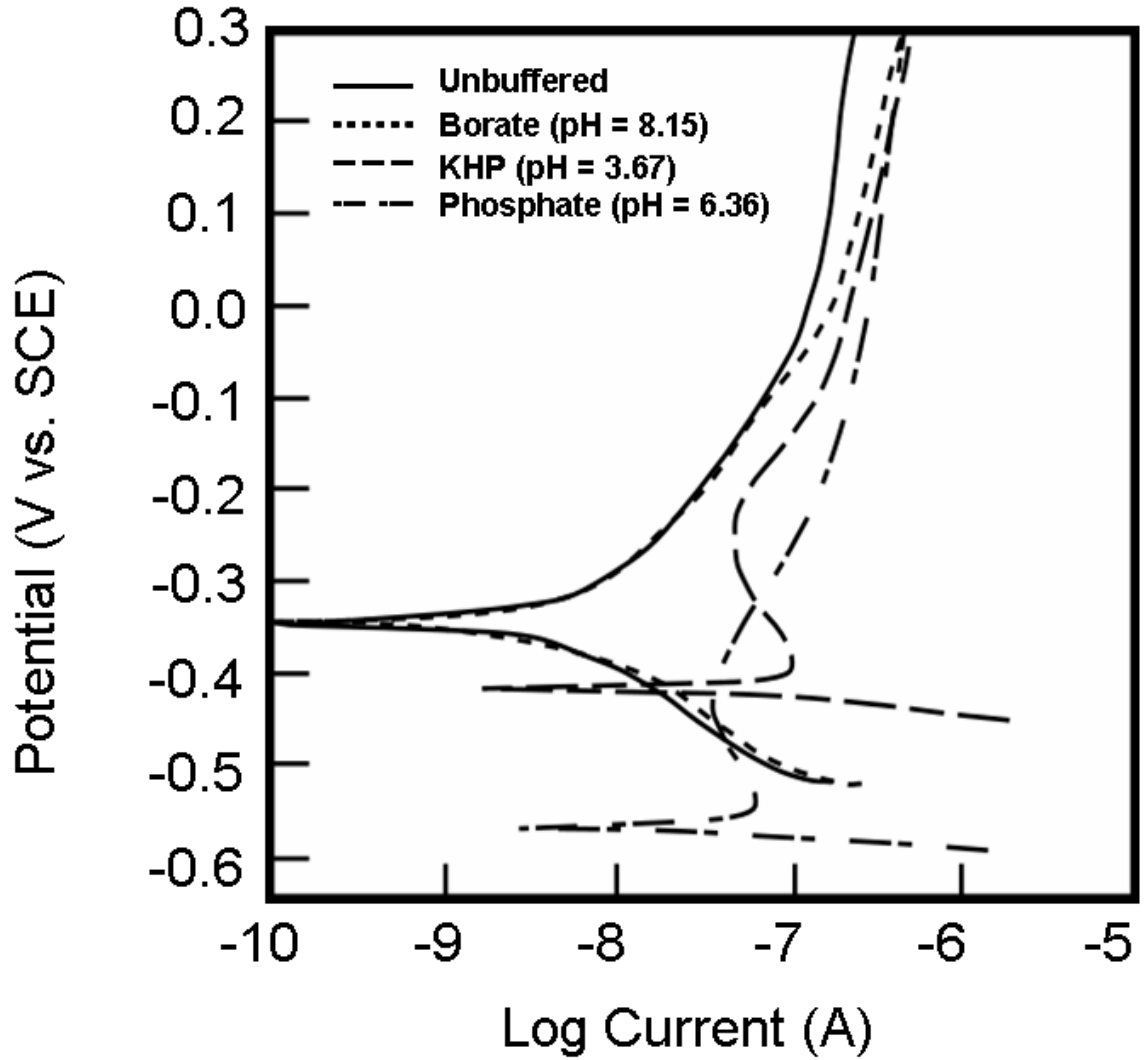

Fig. 4. Potentiodynamic polarization curves for Alloy 22 containing non-implanted elements in deaerated 1 M NaCl solutions with different pH buffers. Samples do not have S or Ar in them. Scan rate was 1 mV/s.

Fig. 5

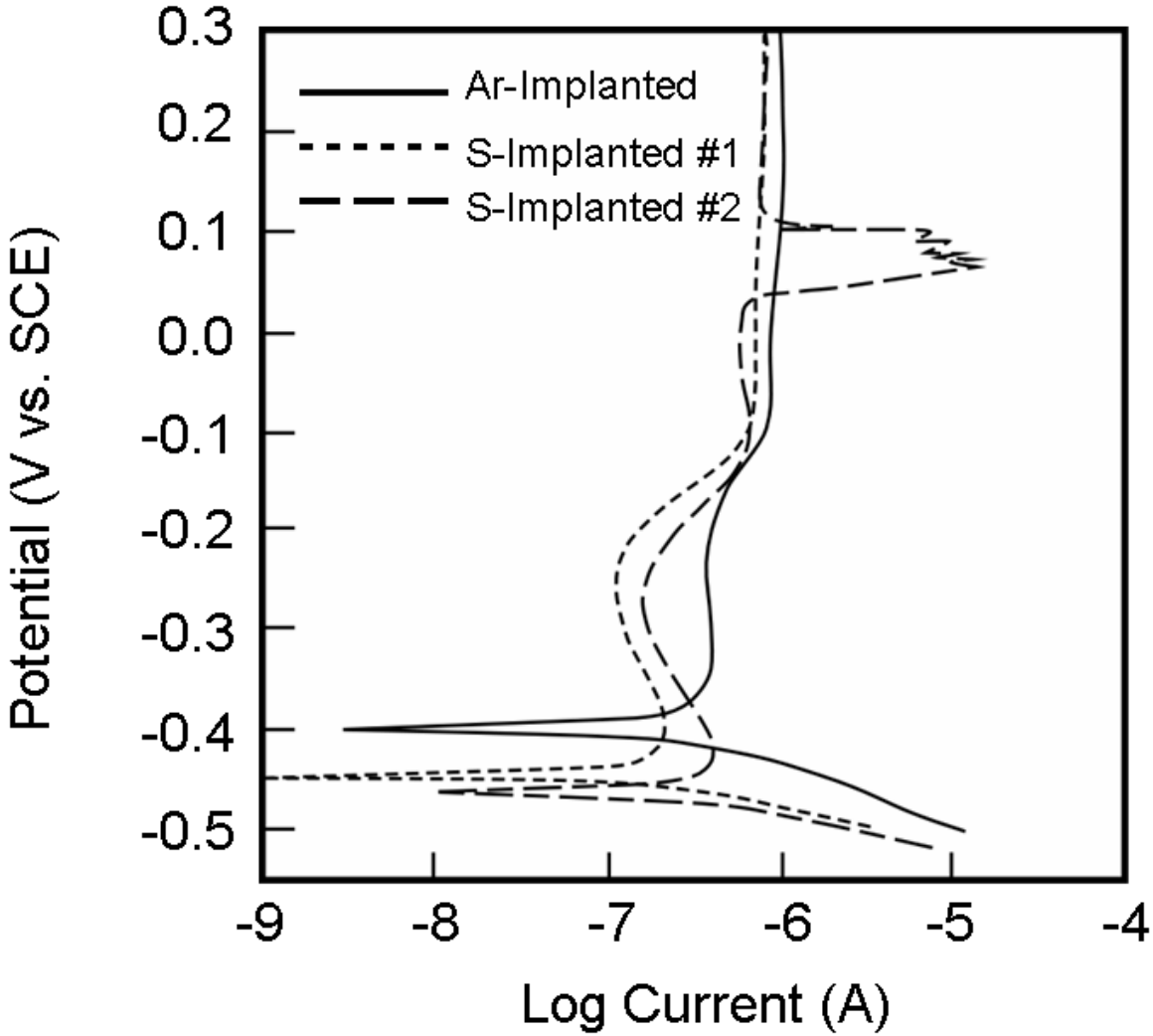

Fig. 5. Potentiodynamic polarization curves for Alloy 22, implanted with Ar and S (duplicate runs for S) and subsequently sputtered to the implant-concentration maximum, in deaerated 1 M NaCl solutions buffered to pH = 3.67 with KHP.

Fig. 6

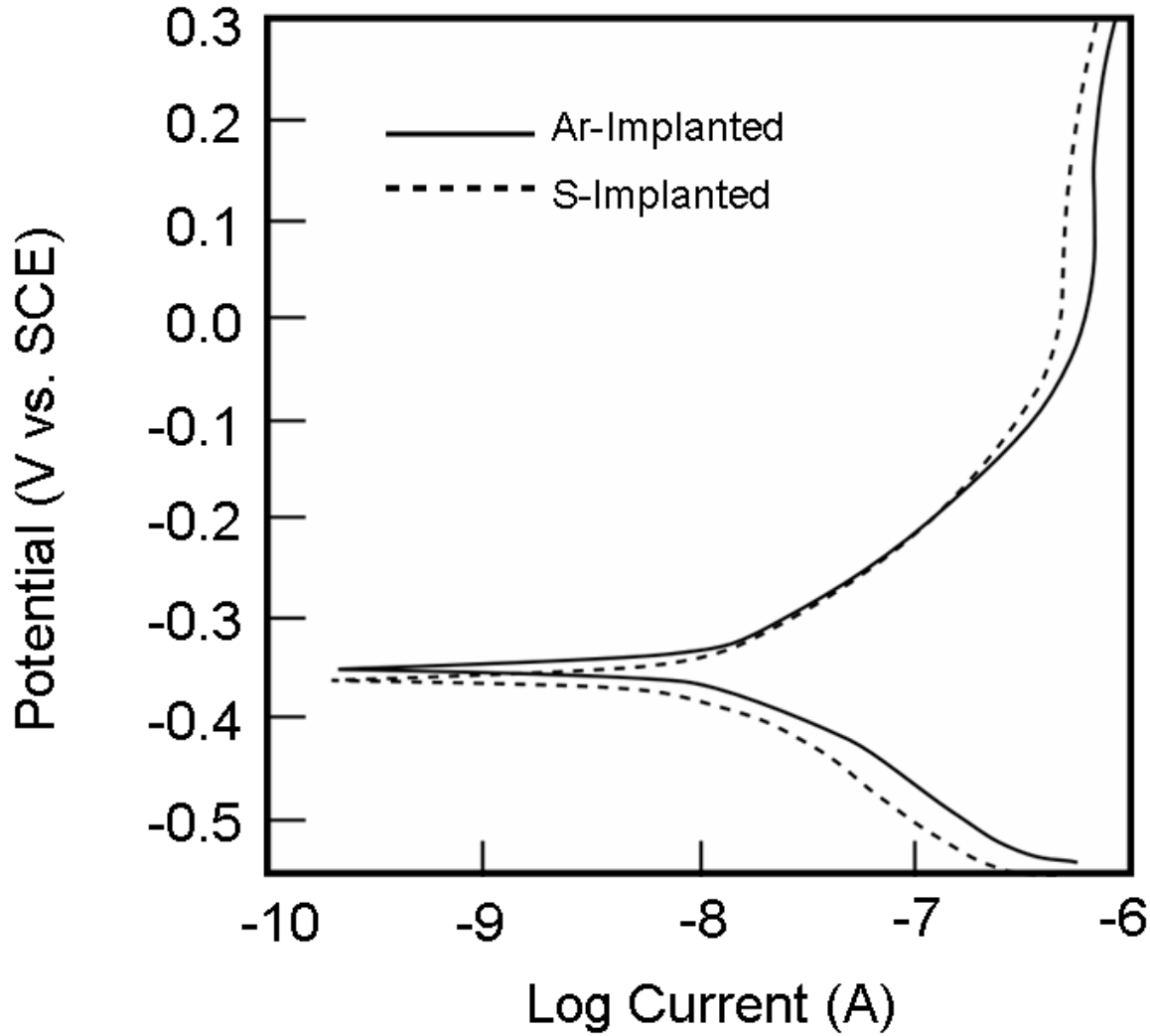

Fig. 6. Potentiodynamic polarization curves for Alloy 22, implanted with Ar and S and subsequently sputtered to the implant-concentration maximum, in deaerated 1 M NaCl solutions buffered to pH = 8.15 with borate.

Fig. 7

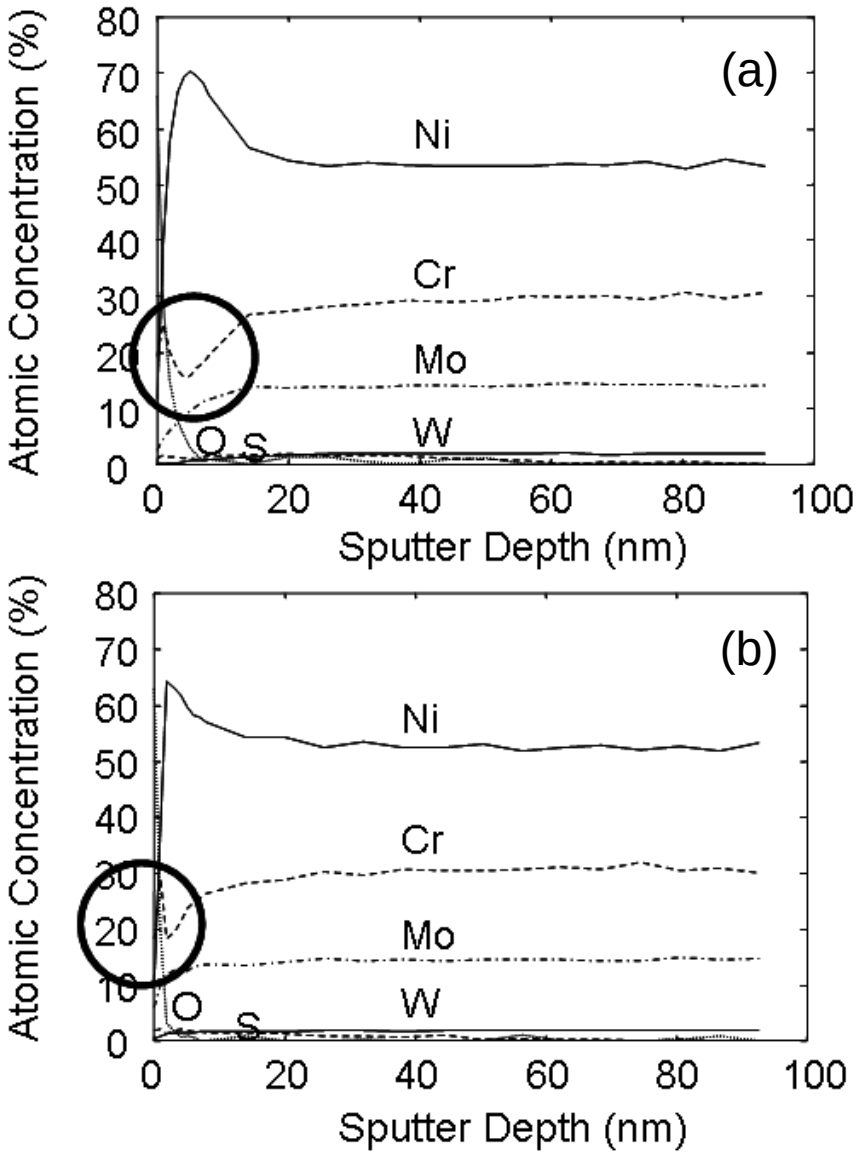

Fig. 7. XPS depth profile for S-implanted Alloy 22 samples (a) as-received and (b) after sputtering with Ar ions (to achieve approximately the S-concentration maximum at the surface), followed by equilibration at the corrosion potential for 1 h and electrochemical polarization. This scale shows the variation of Cr concentration near the surface.

Fig. 8

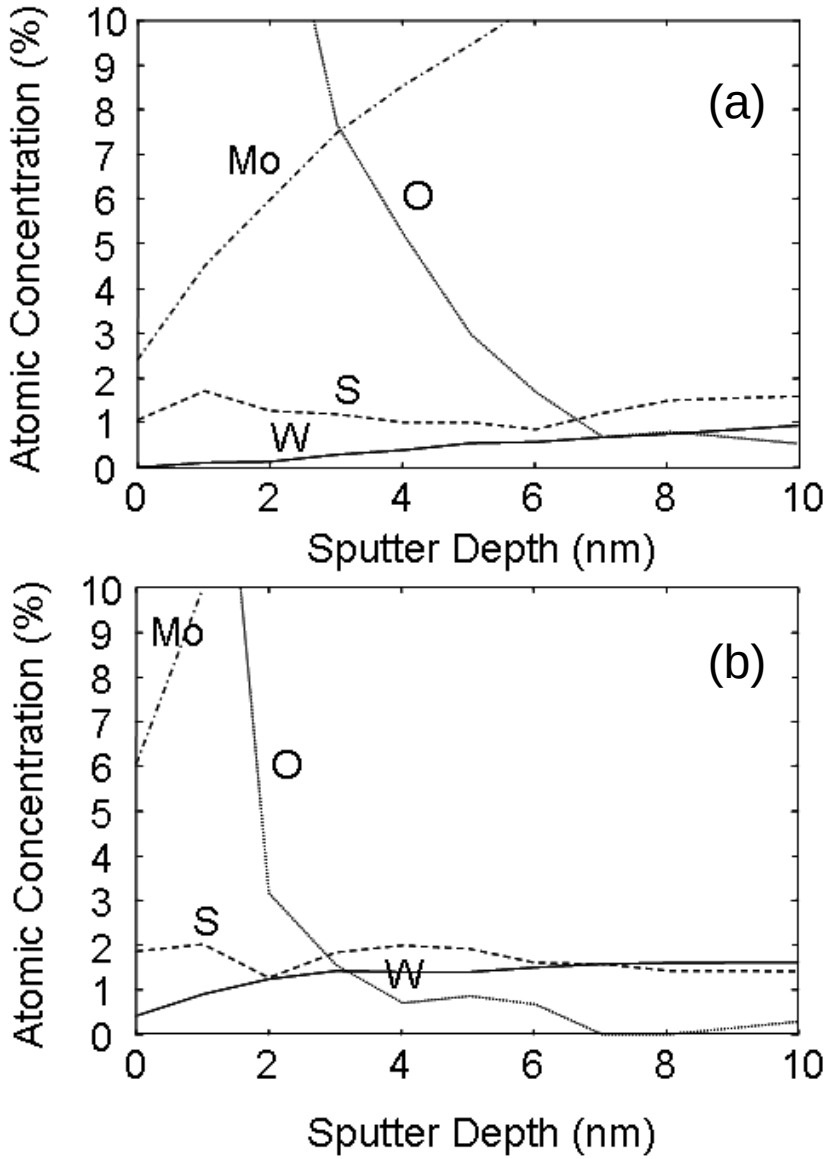

Fig. 8. XPS depth profile for S-implanted Alloy 22 samples (a) as-received and (b) after sputtering with Ar ions (to achieve approximately the S-concentration maximum at the surface), followed by equilibration at the corrosion potential for 1 h and electrochemical polarization. This scale shows variations closer to the surface than Fig. 7.

Fig. 9

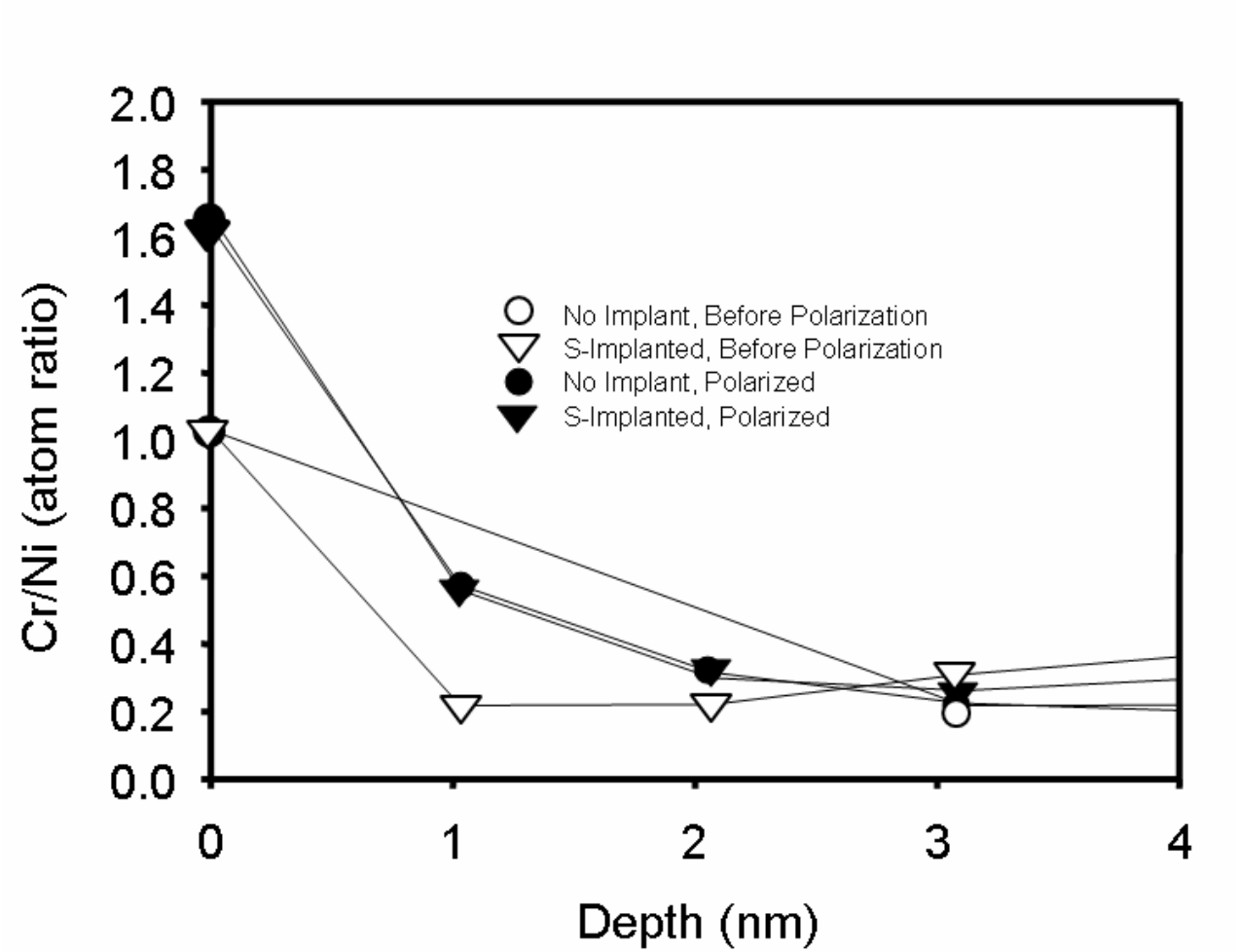

Fig. 9. Variation of the Cr/Ni atom ratio near the surface for different Alloy 22 samples.

Fig. 10

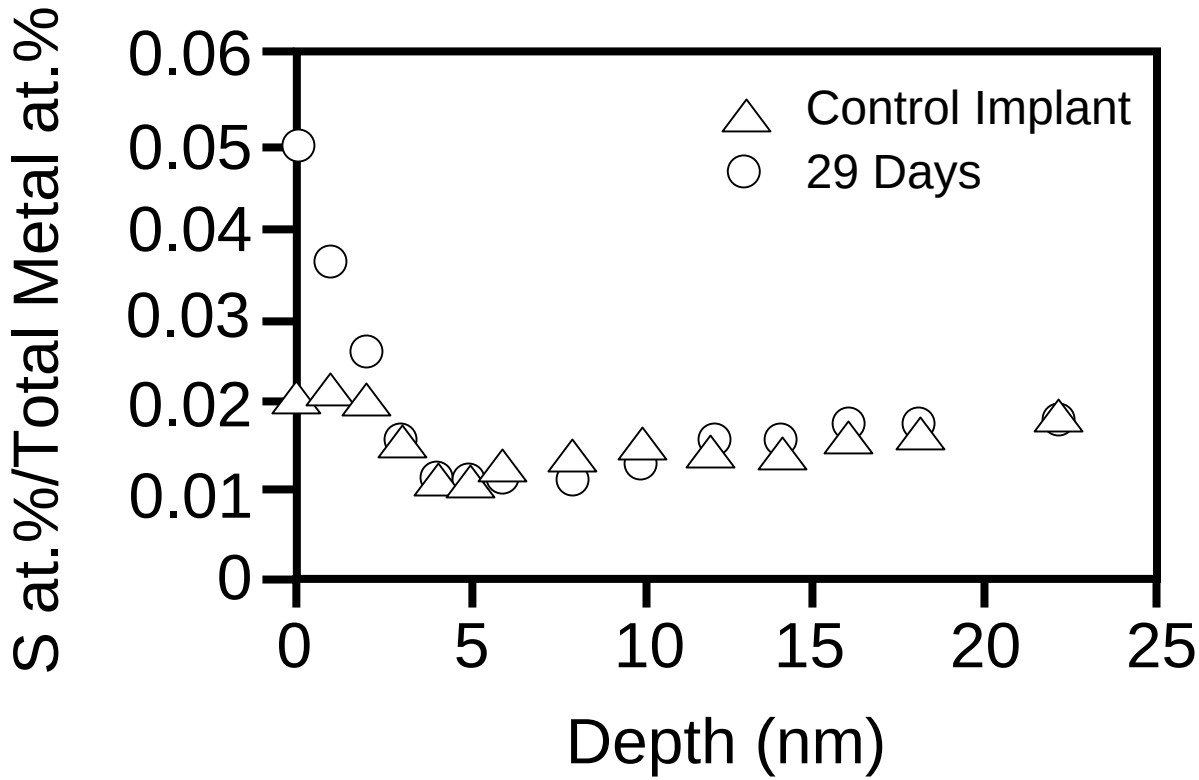

Fig. 10. Depth profile showing the ratio of S-to-metal concentrations as a function of depth for a control sample (S-implant) and S-implanted sample exposed to solution for 29 days. An excess amount of S was accumulated in the surface region of the sample during the 29 days in solution.